

# Preclinical Evaluation of Bone Marrow Mesenchymal Stem Cells Overexpressing MicroRNA-126 to Treat Critical Limb Ischemia

**Pegah Nammian**

Shiraz Medical School: Shiraz University of Medical Sciences <https://orcid.org/0000-0001-7967-0338>

**Seyedeh-Leili Asadi-Yousefabad**

Yazd University of Medical Science: Shahid Sadoughi University of Medical Sciences and Health Services

**Sajad Daneshi**

Shiraz Medical School: Shiraz University of Medical Sciences

**Jafar Fallahi**

Shiraz Medical School: Shiraz University of Medical Sciences

**Seyed Mohammad Bagher Tabei**

Shiraz Medical School: Shiraz University of Medical Sciences

**Vahid Razban** (✉ [razban\\_vahid@yahoo.com](mailto:razban_vahid@yahoo.com))

Department of Molecular Medicine, School of Advanced Medical Sciences and Technologies, Shiraz University of Medical Sciences, Shiraz, Iran

---

## Research

**Keywords:** Therapeutic angiogenesis, Mesenchymal stem cell therapy, gene therapy, microRNA-126, critical limb ischemia

**Posted Date:** June 30th, 2021

**DOI:** <https://doi.org/10.21203/rs.3.rs-653222/v1>

**License:** © ⓘ This work is licensed under a Creative Commons Attribution 4.0 International License.

[Read Full License](#)

---

# Abstract

**Background:** Critical limb ischemia (CLI) considered as the most severe form of peripheral artery disease (PAD), and characterized by ischemic rest pain and non-healing ulcers. CLI being associated with a high risk of major amputation, cardiovascular events and death. Current therapy for CLI are surgical reconstruction and endovascular therapy or limb amputation (for patients with no treatment options). Neovascuogenesis induced by stem cells including mesenchymal stem cells (MSCs) therapy is a promising approach to treat CLI. But this method of treatment faces challenges that reduce its effectiveness, such as: MSCs survival and paracrine secretion. MicroRNAs are post transcriptional regulatory molecules that regulate many biological processes including VEGF pathway. Therefore, microRNAs could be used to increase viability and angiogenic potential of MSCs. This study was conducted to reinforce and increase the angiogenic potential of BM-MSCs by using microRNA-126 and evaluate the effect of this stem cell gene therapy on treatment of ischemic tissues in CLI mouse models.

**Results:** Our cellular, molecular and functional tests indicated that during 28 days after transplantation, BM-MSCs and virus groups had an enhancing effect on angiogenesis. BM-MSCs<sup>miR-126</sup> group had remarkable effect on endothelial cell migration, muscle restructure, functional improvements and neovascularization in ischemic tissues and led to more effective treatment. On the other hand, miR-126 could increase paracrine secretion of BM-MSCs. Additionally, in vivo evaluation showed that miR-126 could increase BM-MSCs survival and paracrine secretion of angiogenic factors such as VEGF, and led to remarkable functional improvements and neovascularization in ischemic tissues.

**Conclusion:** According to the obtained results, it could concluded that combination of BM-MSCs and miR-126 leads to more effective recovery from critical limb ischemia compared to using them alone. In fact, miR-126 can be used as a strong modifier to reinforce the angiogenic potential of BM-MSCs, leading to more effective treatment for CLI.

## Background

Critical limb ischemia (CLI) is the most severe manifestation of peripheral arterial disease (PAD). CLI is the result of PAD with spoiled blood flow in peripheral tissues (1, 2). The first-line treatment is revascularization. Revascularization may be surgical via bypass or endovascular techniques. In the absence of revascularization, up to 40% of patients will require lower limb amputation by 1 year (3). Also, nearly half of patients are not suitable for revascularization procedures because of undesirable endovascular anatomy and high operative risk (4, 5). Today, the use of stem cell therapy (SCT) and gene therapy (GT) in order to stimulate angiogenesis emerged as a promising treatment for disorders related to limb ischemia. The concept of “therapeutic angiogenesis” for CLI, performed by gene, protein, and cell therapy, has recently raised an excellent deal of hope for CLI patients who cannot undergo standard treatment (6, 7). In fact the new proposal for CLI treatment is using growth factors to stimulate formation of new vessels and/or remodeling of dysfunctional vessels. These factors, which are proteins, can be

administered in their protein form, or through genes or cells that express these factors and the treatment modality is known as therapeutic angiogenesis (6, 7).

Gene therapy (GT) represents a promising alternative treatment for CLI. In fact, expression of specific angiogenic growth factors is induced in the ischemic tissue to achieve a more sustained local delivery (8). The genes usually used for angiogenic therapy include the genes for vascular endothelium growth factor (VEGF), fibroblast growth factor (FGF), hepatocyte growth factor (HGF), Stromal Derived Factor-1 (SDF-1), and hypoxia inducible factor (HIF-1) (9). Gene therapy faces with some important challenges, including: 1) delivery route 2) duration of gene expression 3) complexity of angiogenesis process: in fact, formation of new blood vessels is a complex process that involving proliferation and differentiation of precursor cells under the control of many regulatory molecules. Thus, using a single factor that specifically acts on endothelial cells is possibly insufficient to form a mature vessel in an ischemic and inflamed environment (10, 11).

Stem cell therapy (SCT) shows a grate promising alternative treatment for CLI. Whereas SCs play an important role in neovascularization process, the therapy involving these cells can theoretically be more efficient compared with the protein or gene therapy due to their direct self-renewal and differentiation into an organ-specific cell, and also to their paracrine effect (6, 12, 13). Numerous trials have tested the administration of mesenchymal stem cells (MSCs) for treatment of CLI. The characteristics that make these cells ideal for this application are, ease of isolation and expansion, low immunogenicity in allogeneic settings, differentiation to specific cells, and ability to secrete paracrine factors that stimulate regeneration, demonstrated safety, and tropism toward sites of hypoxia (14-16). While MSCs therapy have shown great results in animal models, the finite success in human clinical trials indicates that more potent treatment strategies or cell formulations are needed. In fact, by combining cell and gene therapy, MSCs that are genetically modified to over express angiogenic genes could be an optimal approach, for treatment of CLI (11, 17).

Investigations about stem cell therapy for CLI focus on the use of bone marrow mesenchymal stem cells (BMSCs), and support by various clinical evidences (18, 19). Mesenchymal stem cells (MSCs) consist of nearly 0.001% to 0.08% of cells within bone marrow and are nonhematopoietic stromal cells be able to differentiate into mesenchymal lineages, such as muscle, bone, cartilage and fat. They can be culture-expanded easily to harvest a large number of cells. In addition these cells can be stored for both autologous and allogeneic use (20). In multiple preclinical studies, the therapeutic angiogenesis of BMSCs were proved and also there are strong evidences that BMSCs have the potential to produce growth factors, angiogenesis-related cytokines, chemokines and extracellular matrix molecules, and also have similar cellular and molecular properties with pericytes (14, 21).

Although, stem cell therapy (SCT) faces with some important challenges, including: 1) identify the most ideal cell type 2) standardization of procedures of MSC isolation and expansion 3) in vivo administration route 4) dosage optimization 5) survival of the cells 6) administration timing (22, 23).

MicroRNAs (miRNAs) are a class of small (~18–22 bp), endogenous single-stranded and non-coding RNA molecules with conserved structures. They constitute nearly 1% to 2% of the eukaryotic transcriptome. MicroRNAs have significant roles as posttranscriptional gene regulators in different cellular processes such as, cell proliferation, apoptosis, differentiation of cells including endothelial cells (ECs) and stem cells, metabolism, tissue homeostasis, embryonic development and even tumor formation (24, 25). The biologic roles of miRNAs in vascular diseases have led to an increased interest in miRNA regulation as a therapeutic and diagnostic approach. Recent studies demonstrated that miRNAs show promising potential in therapeutic interventions directed toward ischemic diseases (26, 27).

Several specific miRNAs have been identified as angiogenic regulators, including miRNA-126 (miR-126). MicroRNA-126 is a major positive regulator of vascular integrity and angiogenic signaling in vivo, in fact it has a distinguished role in the control of vascular integrity and angiogenesis through distribution of angiogenic factors, such as vascular endothelial growth factor (VEGF), Hypoxia Inducible Factor 1-alpha (HIF-1 $\alpha$ ), and matrix metalloproteinase (MMPs) (28). As a matter of fact one of the most vigorous microRNA functions on angiogenesis is revealed by microRNA-126 (29, 30). MicroRNA-126-3p and microRNA-126-5p are the two mature strands of the pre-microRNA-126 that have cell-type and strand-specific function in angiogenesis. MicroRNA-126 regulates the response of ECs to angiogenic factors such as VEGF, through directly repressing negative regulators of VEGF pathway, including the Sprout-related EVH1 domain-containing protein 1 (SPRED1) and phosphoinositol-3 kinase regulatory subunit 2 (PIK3R2/p85-b), miR-126 regulates SPRED1 and PIK3R2 by directly targeting the 3-UTR (31, 32).

The ideal angiogenic treatment for limb ischemia would be one that can act on all or a majority of the cells and molecules that participate in angiogenesis and control of inflammation. Some ways to achieve this ideal treatment are: 1. using more angiogenic genes 2. using genetically modified stem cells (9, 11).

The purpose of this study was to reinforce the angiogenic potential of Bone Marrow Mesenchymal Stem Cells (BM-MSCs) by using miR-126. According to the previous studies new therapeutic ways to treat CLI including gene therapy and stem cell therapy, facing with some critical challenges that cause these methods do not have acceptable results in treating CLI. On the other hand, using these methods alone will not show the desired results. It seems that due to the gene regulatory potential of miR-126 and angiogenic potential and also its effects on BM-MSCs functions and survival, the use of miR-126 and BM-MSCs as a combination therapy will have better results in CLI treatment.

## Methods

### MicroRNA design

In order to evaluate the angiogenic potential of miR-126, shRNA-lentiviral vector construct was made. At first step shRNA was designed. In the present study, annealed oligos method was used. However, some changes were made in the shRNA design according to the purpose of the study. The entire procedure involves the following steps:

1. The sequence of miR-126-3p and miR-126-5p was determined according to sequences from <http://www.mirbase.org/>. The 3p arm of shRNA is known as guide strand and the 5p arm is known as passenger strand. The shRNA sequence (from 5' to 3') will be in the order of passenger strand, loop, and then guide strand.

MiR-126-3p sequence: 5'-UCGUACCGUGAGUAAUAAUGCG-3'

MiR-126-5p sequence: 5'-CAUUAUUACUUUUGGUACGCG-3'

2. A sixth nucleotide loop was set to connect 3p and 5p strands.

Loop sequence: CTCGAG

3. In order to clone the shRNA to pLKO.1-TRC vector the complementary sequences of restriction endonuclease Age1 and EcoR1 enzymes were designed at the 5' ends of the oligonucleotides.

4. According to the mentioned points the sequence of the two oligos will be as follows:

Forward oligo: 5' CCGG-21bp 5p strand-CTCGAG-21bp 3p strand-TTTTTG 3'

Reverse oligo: 5' AATTCAAAA-21bp 5p strand-CTCGAG-21bp 3p strand 3'

### **BM-MSCs isolation and culture**

To isolate bone marrow, 6-week-old C57BL/6 mice were killed by cervical dislocation, then the ends of tibia and femur bones were cut to expose the marrow. 5-ml syringe containing complete media used to extract the cells via flushing the marrow plug out of the cut end of the bone with 1 ml of complete media and collect in a 15-ml tube. Strong flushing is necessary during marrow cell preparation. Then the cell pellet derived from 2 tibia and 2 femur bones was suspended in growth medium containing Dulbecco's modified Eagle's medium (DMEM) high glucose (Gibco, USA) and 10% fetal bovine serum (FBS; Gibco, USA) with 100 U/mL penicillin-streptomycin (Gibco, USA) and cultured in a 75-cm<sup>2</sup> culture flask and were maintained at 37C and 5% CO<sub>2</sub>. Nonadherent cells were removed after 24 h and the flask was washed with phosphate-buffered saline (PBS; Gibco, USA). The medium was changed regularly every 3-4 days, and at approximately 70% confluence, the cells were detached using trypsin-EDTA (Gibco, USA) and transferred to new flasks, these cells were considered as passage 1(Figure 1).

### **Differentiation of BM-MSCs**

Osteogenesis: for differentiation to osteocyte, passage 3 BM-MSCs were incubated to differentiate into osteoblasts in corresponding induction medium for 2 weeks. The cells were maintained in control and osteogenic media. The control medium consisted of DMEM (Gibco, USA), supplemented with 10% FBS (Gibco, USA), 1% penicillin/streptomycin (Gibco, USA). The osteogenic medium contained DMEM, 15% FBS (Gibco, USA), 100 µM L-ascorbic acid, 10 mM glycerol 3-phosphate, and 100 nM dexamethasone (Sigma-Aldrich). Medium was replaced 2 times a week. After 2 weeks the cultured cells were stained with

Alizarin Red solution to visualize calcium deposits. The cells were fixed in 4% paraformaldehyde (PFA) for 20 minutes and stained using Alizarin Red solution for 20 minutes at room temperature.

**Adipogenesis:** for Adipocyte differentiation passage 3 BM-MSCs were incubated to differentiate into adipocytes in corresponding induction medium for 2 weeks. The cells were maintained in control and Adipogenic media. The control medium consisted of DMEM (Gibco, USA), supplemented with 10% FBS (Gibco, USA), 1% penicillin/streptomycin (Gibco, USA). The Adipogenic medium contained DMEM, 15% FBS, 100  $\mu$ M L-ascorbic acid, 200  $\mu$ M Indomethacin, 1000 nM insulin (Sigma-Aldrich) and 100 nM dexamethasone (Sigma-Aldrich). Medium was replaced 2 times a week. After 2 weeks the cultured cells were stained with Oil Red-O solution to visualize lipid vacuoles. The cells were fixed in 4% paraformaldehyde (PFA) for 20 minutes and stained using Oil Red-O solution for 20 minutes at room temperature.

### Flow cytometry analysis of MSCs

For the analysis of surface marker expression of BM-MSCs Flow cytometry was performed. The expression of surface markers was evaluated using monoclonal antibodies against mouse anti-CD44 FITC, anti-CD105 perCP, anti-CD45 FITC, and anti-CD34 PE. The cells at passage 4 were washed with PBS, and then harvested via incubation in 0.05% trypsin/EDTA. After centrifugation, the cell pellets were washed with PBS and resuspended in 1 ml PBS. Then the cells were stained with the specific antibodies in darkness. After incubation for 30 minutes at 4 °C, the cells were washed with PBS, and then analyzed by flow cytometry. The data was analyzed with Flow Jo software (version 7.6).

### Lentivirus production and titration

In the present study we used second generation self-inactivating (SIN) human immunodeficiency virus-1-based (HIV-1), VSV-G pseudotyped lentiviral vectors. Second generation LVs were produced by calcium phosphate-mediated transfection into 293T cells. Briefly, packaging plasmid psPAX2 (Addgene plasmid 12260), envelope plasmid pMD2.G (Addgene plasmid 12259) and transfer plasmid pLKO.1-TRC (Addgene plasmid 10878) were transfected into 293T cells using Ca<sub>3</sub>PO<sub>4</sub> transfection protocol. Culture medium was replaced 6 h post-transfection. Vector-containing supernatants were collected 24, 48 h, and 72 h post-transfection, and concentrated by Amicon filter 100 MW. Lentivirus vector titer was determined on 293T cells and vector particles were measured by puromycin titration. Vector aliquots were stored at -80°C.

### Transduction of BM-MSCs and puromycin reporter gene detection

Cells were seeded in six-well plates at  $5 \times 10^4$  cells per well and different concentrations of virus were added and incubated at 37°C for 72 h. The volume of lentivirus to be used was determined from titer results. After incubation, 1.5 mL of fresh DMEM complete containing 2  $\mu$ g puromycin (Sigma) was added to each well. It was the beginning of the selection process. After 2 days, the culture medium was removed

from each well and fresh medium was added without puromycin. The resistant cells (stable cell line) were cultured and expanded into T75 flask.

#### Cell migration assay (wound healing assay)

Wound-healing assay on endothelial cells, human umbilical vein endothelial cell (HUVECs), was used to study the paracrine effect of BM-MSCs and BM-MSCs miR-126 on endothelial cell migration potential. After 24-h FBS starvation of MSCs, the supernatants from cells were collected. The wound-healing assay was employed by scratching the monolayer HUVEC confluent cell cultures using a sterile plastic micropipette tip. The cells were washed by DMEM and PBS twice for smoothing the edges of the scratch and removing floating cells. After that, wound healing initiated by adding the collected supernatants from BM-MSCs and BM-MSCs miR-126 on HUVEC cultures in different wells of a 6-well plate. After incubating the cells at 37 °C in 5% CO<sub>2</sub> for 0, 15, 18, 20, 22 and 24 h, the migration images of the cells were observed under a microscope with 10x (Nikon, ECLIPSE, TS100), the distance of cell migration was measured and images taken using image-J Analysis software.

#### Mouse Critical limb Ischemia model

All animal experiments were performed according to the guidelines approved by the Shiraz University of Medical Sciences ethics committee (1397.430).

Male C57BL/6 mice, weighing 25–30 g (6–8 week-old) purchased from Comparative and Experimental Medicine center at Shiraz University of Medical Sciences and were selected randomly. Animals were kept in standard conditions (12 h light and 12 h darkness, temperature of 18–22 °C, and 55 ± 5% humidity). They were fed standard mouse diet and given water ad libitum.

For creating critical limb ischemia (CLI) model, all animals in each group were anesthetized intraperitoneal (IP) administration using ketamine 10% (100 mg/kg, Alfasan CO., Netherlands) and xylazine 2% (5 mg/kg, Alfasan CO., Netherlands). Animals were placed in dorsal recumbency. A skin incision (about 10 mm) was done along the center of the medial thigh from the abdomen towards the knee. Subcutaneous fat tissue superficial was gently pushed away to exposed femoral neurovascular bundle. The femoral artery pushed away from the femoral vein and nerve. Subsequently, the femoral artery was isolated by blunt dissection from the femoral vein at the ligation sites between the proximal caudal femoral artery and the bifurcation of the deep femoral artery and saphenous artery. Then two sutures were passed using 6-0 silk, transected and cauterized. The incision was closed using continues 5-0 vicryl sutures. The operation was done under a surgical microscope (Zeiss OP-MI6 SD; Carl Zeiss, Goettingen, Germany) (Figure 2).

#### Animal groups and transplantation

The male mice were randomly divided into the following four groups (n=12/group): (1) control group: CLI was performed and received PBS into ischemic site, (2) BM-MSCs group: CLI was performed and received BM-MSCs, (3) virus-miR-126 (recombinant vector) group: CLI was performed and received recombinant

vector, (4) BM-MSCs<sup>miR-126</sup> group: CLI was performed and received BM-MSCs that transfected with virus-miR-126. To transfer the cells and recombinant vector into ischemic leg, intramuscularly (IM) injection of  $5 \times 10^5$  BM-MSCs and BM-MSCs<sup>miR-126</sup> that resuspended in PBS and  $4.7 \times 10^6$  virus particles as treatment groups and PBS as a control group were done at four different sites of gastrocnemius (GC) muscle 24 hours after surgery.

Additionally to identify the presence of grafted BM-MSCs and BM-MSCs<sup>miR-126</sup> in the gastrocnemius (GC) muscle the fifth and sixth groups were added as, survival groups: CLI was performed on female mice (n=5/group) and received intramuscularly (IM) injection of  $5 \times 10^5$  male BM-MSCs and BM-MSCs<sup>miR-126</sup> at four different sites of gastrocnemius (GC) muscle 24 hours after surgery.

### **Functional scoring**

Functional grading was performed according to the Tarlov, ischemia, modified ischemia, function and the grade of limb necrosis scoring system at pre-operation, post-operation and at days 3, 7, 14, 21 and 28 after transplantation. The degree of ischemic damage was evaluated through indicators, such as skin color changes, swelling, and grade of the limb necrosis (Table 1).

### **Investigation of donor cell survival**

To identify the presence of grafted male cells in the female gastrocnemius (GC) muscle (the survival groups), the Y chromosome-specific SRY gene was assessed by polymerase chain reaction. At days 3, 7, 14, 21, and 28 after treatment, the GC muscle was collected, genomic DNA was extracted using Trizol (Sigma-Aldrich) and then SRY analysis was performed by PCR. The forward primer sequence was 5'-TTTATGGTGTGGTCCCGTGGTGAG-3' and the reverse primer sequence was 5'-TTGGAGTACAGGTGTGCAGCTCTAC-3'.

### **RNA isolation and quantitative real-time PCR**

In order to evaluate the expression of target genes (VEGF, SPRED1, PIK3R2 and GAPDH as housekeeping gene), after transplantation at days 7, 14, 21 and 28, the GC muscle was collected, total RNA was extracted using Trizol (Sigma-Aldrich T9424) according to the manufacturer's protocol. The concentration of total RNA was quantified by the absorbance at 260 nm. Extracted RNA was then reverse-transcribed using the SMOBIO cDNA Synthesis Kit RP1300. Then gene expression analysis was performed by Real-time PCR. qRT-PCR was performed on an ABI Prism 7500 PCR system using RealQ Plus 2X Master Mix Green Low Rox (Amplicon). PCR was performed in a total reaction volume of 15 ml consisting of appropriate cDNA. For semi-quantitative RT-PCR, the following primers were used (Table 2).

The two-step reaction was performed triplet for all samples. The PCR was performed under the following cycling conditions: denaturation at 95 °C for 15 min, followed by 40 cycles of 30 sec at 95°C and 30 sec at 62°C (annealing), and extension at 72 °C for 30 sec. Data were analyzed by the comparative cycle threshold (Ct) method and normalized against GAPDH controls.

## Histopathological evaluation

Histological analysis of limb tissues were done at days 7, 14, 21 and 28 after transplantation. To evaluate that the target cells (BM-MSCs and BM-MSCs<sup>miR-126</sup>) and recombinant vector can induce angiogenesis in the gastrocnemius muscle, immunohistologic staining was performed with an anti-CD31 antibody (Biocare Medical), a marker for vascular endothelial cells. The mice were euthanized at predetermined times and gastrocnemius was removed and fixed in 10% formalin. After fixation, the tissue was embedded in paraffin, and the tissue sections were prepared and mounted on slides. Then tissue section slides were stained with hematoxylin-eosin (H&E) and assessed by microscopy (Olympus BX43, Shinjuku, Japan). The tissue samples were deparaffinized by xylene and ethanol and then antigen retrieval was performed with proteinase K treatment. After this treatment, the tissue samples were incubated with an anti-CD31 monoclonal primary antibody at 100  $\mu$ L for 15 minutes at room temperature. After being washed with TBS, the samples were incubated with a master polymer plus HRP at room temperature for 30 minutes. Then samples were washed with TBS. Chromogen solution was prepared, 1 drop of DAB Chromogen concentrate to 1 ml of DAB substrate buffer. Samples were treated with DAB and incubated at room temperature for 5 minutes. The samples were covered with hematoxylin for 15 seconds and then washed with distilled water. After that dehydration step was performed by alcohol solutions at room temperature for 30 seconds. Finally the samples was cleared in xylene and mounted with permanent mounting medium. Tissue sections were analyzed using the vascular hotspot technique to obtain MVD. Sections were scanned at low power to determine areas of highest vascular density. Within this region, individual microvessels were counted in three separate random fields at high power (0.142-mm<sup>2</sup> field size). The mean vessel count from the three fields was used. A single countable microvessel was defined as any endothelial cell or group of cells that was clearly separate from other vessels, stroma, or tumor cells without the necessity of a vessel lumen or RBC within the lumen. Areas of gross hemorrhage and necrosis were avoided. MVD counts were measured by counting CD31 IHC hot spots in three separate 400 $\times$  fields.

## Statistical analysis

Statistical analysis was performed using GraphPad Prism 7 Software. Results are expressed as the mean standard error of the mean. Comparisons between multiple groups were performed using one-way analysis of variance (ANOVA), with post hoc testing performed with Bonferroni analysis or unpaired t-tests, as appropriate. Also comparisons between two groups were performed using independent sample T-test. P values  $\leq$  0.05 were considered statistically significant (\*p < .05, \*\*p < .01, \*\*\*p < .001, \*\*\*\*p < .0001). Data were presented as mean  $\pm$  standard deviation (SD).

# Results

## Characterization of BM-MSCs

BM-MSCs were extracted from bone marrow tissue of C57BL/6 mice and at first step spindle-shaped morphology of the cells were evaluated at passage 3 (Figure 3 A). To characterize the phenotypes of BM-MSCs, flow cytometry was performed to analyze the surface markers of MSCs. Cells were labelled with FITC, perCP and PE-conjugated antibodies and were examined by flow cytometry. The cells were dissociated and were stained with CD34, CD45 (hematopoietic cell markers) and CD44, CD105 (mesenchymal stem-cell markers). Results showed that the BM-MSCs were strongly positive for MSC marker CD44 and negative for cell markers CD105, CD34 and CD45 (Figure 3 B-E).

### **Differentiation capacities of BM-MSCs**

The differentiation capacities of BM-MSCs to osteocyte and adipocyte were obtained using Alizarin Red staining and Oil Red-O staining, respectively. Alizarin Red staining showed that after 2 weeks, mineralized nodules formed in the BM-MSCs under the osteogenic induction. Additionally, Oil Red-O staining demonstrated that lipid-rich vacuoles formed after 2 weeks under the adipogenic induction (Figure 4 A, B).

### **Capacity of BM-MSCs and BM-MSCs<sup>miR-126</sup> supernatant in cell migration**

Scratch assay was performed on the target cells. The results showed that BM-MSCs and BM-MSCs<sup>miR-126</sup> supernatant led to increased migration potential of endothelial cells (HUVECs) through a paracrine manner. The supernatant of both cells led to the complete closure of the wound after 24 h. At time points 15, 18, 20, 22 and 24 h post-scratch, we documented a significant percentage decrease in the scratch area remaining between the BM-MSC compared to the control group (19.44±0.61, 13.5±0.33, 10.59±0.5, 5.37±0.25, 0±0, respectively,  $p < 0.0001$  for all time points). Additionally, at time points 15, 18, 20, 22 and 24 h post-scratch, the BM-MSCs<sup>miR-126</sup> group showed a significant decrease in scratch area remaining compared to the control group (15.33±0.4, 10.5±0.4, 6.2±0.2, 3.6±0.4, 0±0, respectively,  $p < 0.0001$  for all time points). In fact supernatants from both cell sources showed remarkable effect in cell migration compared with the control group, although BM-MSCs<sup>miR-126</sup> group effect was better than BM-MSCs group. For the control group, no scratch was 100% healed by the end of the 24 h experiment. The Photos taken with a microscope in a time series then analyzed by image J software in order to calculate the distance between gaps (Figure 5).

### **Evaluation of the recovery of damaged limbs after transplantation**

In order to test the in vivo function of virus, BM-MSCs and BM-MSCs<sup>miR-126</sup> in ischemic hindlimb injury, the day after surgery mice were treated with PBS as control group and  $5 \times 10^5$  BM-MSCs, BM-MSCs<sup>miR-126</sup> and  $4.7 \times 10^6$  virus particles were injected into the gastrocnemius muscle. Muscle strength testing was performed in the gastrocnemius muscle during 28 days after treatment. The activity of limbs was evaluated by Tarlov and Function scores and severity of ischemic changes was evaluated by Ischemia, Modified ischemia and the grade of limb necrosis scores. Results indicated that, all transplanted mice and non-treated mice moved with difficulty after the first day of transplantation, in fact mice did not walk

well and only dragged their feet. Over 28 days, BM-MSCs treated mice showed improved functional outcomes compared with control group, with accelerated improvement in the Tarlov score at days 14 and 21 ( $6\pm 0$ ,  $p < 0.0001$ ,  $5.8\pm 0.44$ ,  $p < 0.0001$ ) and Function score at days 14, 21, and 28 ( $5\pm 0$ ,  $P = 0.006$ ,  $4.8\pm 0.4$ ,  $P = 0.01$ ,  $5\pm 0$ ,  $P = 0.006$ ). In recombinant vector treated mice group the process of recovery was similar to BM-MSCs treated mice group, but it was much better than control group. In fact virus treated mice group had improvements in the Tarlov score at days 14 and 21 ( $5.8\pm 0.4$ ,  $p < 0.0001$ ,  $6\pm 0$ ,  $p < 0.0001$ ) and Function score at days 14, 21, and 28 ( $5\pm 0$ ,  $P = 0.006$ ,  $5\pm 0$ ,  $P = 0.01$ ,  $5\pm 0$ ,  $P = 0.006$ ). In fact the rate of hindlimb recovery was increased in BM-MSCs and also in virus transplanted mice, started at day 14. For BM-MSCs <sup>miR-126</sup> group, the rate of hindlimb recovery was significantly better than BM-MSCs and virus groups. BM-MSCs <sup>miR-126</sup> group had improvements in the Tarlov score at days 3, 7, 14 and 21 ( $5.6\pm 0.5$ ,  $p < 0.0001$ ,  $6\pm 0$ ,  $p < 0.0001$ ,  $6\pm 0$ ,  $p < 0.0001$ ,  $6\pm 0$ ) and Function score at days 7, 14, 21, and 28 ( $5\pm 0$ ,  $P = 0.007$ ,  $5\pm 0$ ,  $P = 0.006$ ,  $5\pm 0$ ,  $P = 0.01$ ,  $5\pm 0$ ,  $P = 0.006$ ). The grade of ischemia improved in BM-MSCs treated mice using the ischemia score at days 14, 21, and 28 ( $5\pm 0$ ,  $p < 0.0001$ ,  $4.8\pm 0.4$ ,  $P = 0.0001$ ,  $5\pm 0$ ,  $P = 0.0002$ ) and the modified ischemia score at days 7 and 14 ( $7\pm 0$ ,  $P = 0.0005$ ,  $7\pm 0$ ,  $p < 0.0001$ ). Additionally, the grade of ischemia improved in virus treated mice using the ischemia score at days 14, 21, and 28 ( $5\pm 0$ ,  $p < 0.0001$ ,  $5\pm 0$ ,  $P = 0.0001$ ,  $5\pm 0$ ,  $P = 0.0002$ ) and the modified ischemia score at days 7 and 14 ( $7\pm 0$ ,  $P = 0.0005$ ,  $7\pm 0$ ,  $p < 0.0001$ ). For BM-MSCs <sup>miR-126</sup> group, the rate of ischemia recovery was significantly faster than other groups. The grade of ischemia improved according to the ischemia score at days 3, 7, 14, 21, and 28 ( $4.6\pm 0.5$ ,  $P = 0.006$ ,  $5\pm 0$ ,  $P = 0.005$ ,  $5\pm 0$ ,  $p < 0.0001$ ,  $5\pm 0$ ,  $P = 0.0001$ ,  $5\pm 0$ ,  $P = 0.0002$ ) and the modified ischemia score at days 7, and 14 ( $7\pm 0$ ,  $P = 0.0005$ ,  $7\pm 0$ ,  $p < 0.0001$ ).

The degree of ischemic damage was assessed through indicators, such as swelling, skin color changes and grade of the limb necrosis. Necrotic changes were macroscopically evaluated using the grade of limb necrosis score, in BM-MSCs and recombinant vector treated mice groups, ischemic damage recovery was observed at day 7 ( $0.4\pm 0.5$ ,  $p < 0.0001$ ) and ( $0\pm 0$ ,  $p < 0.0001$ ) respectively. For BM-MSCs <sup>miR-126</sup> group, no signs of necrosis were observed (Figure 6).

### PCR for SRY gene

Polymerase chain reaction for Y chromosome gene SRY was performed. Results indicated that at days 3, 7, 14 and 21 donor male BM-MSCs and at days 3, 7, 14, 21 and 28 BM-MSCs <sup>miR-126</sup> were survived in GC muscle of female mice. But at day 28 no SRY gene was detected in GC muscle for BM-MSCs cells (Figure 7 A, B).

### MiR-126 overexpression increased VEGF expression, and induced angiogenesis

In order to understand the angiogenic potential of BM-MSCs, recombinant vector and BM-MSCs <sup>miR-126</sup>, gastrocnemius muscles were collected at days 7, 14, 21, and 28 after transplantation and real-time PCR was performed to determine the expression of VEGF.

The analysis of VEGF expression indicated that in BM-MSCs treated mice group expression of VEGF increased at days 14, 21, and 28 compared with control group, starting from day 14 ( $7.3 \pm 0.6$ ,  $5.8 \pm 0.2$ ,  $2.8 \pm 0.2$ ,  $p < 0.0001$  for all time points). Additionally results indicated that recombinant vector group compared to BM-MSCs group had similar effect on VEGF expression and had great effect compared to control group. In fact VEGF expression was increased at days 14, 21, and 28 starting from day 14 ( $6.6 \pm 0.4$ ,  $p < 0.0001$ ,  $5.7 \pm 0.5$ ,  $p < 0.0001$ ,  $2.9 \pm 0.4$ ,  $P = 0.001$ , respectively). BM-MSCs<sup>miR-126</sup> group showed significant VEGF expression compared to other groups, at days 7, 14, 21, and 28 starting at day 7 ( $6.3 \pm 0.6$ ,  $p < 0.0001$ ,  $9.4 \pm 0.5$ ,  $p = 0.001$ ,  $7.2 \pm 0.6$ ,  $P = 0.02$ ,  $4.2 \pm 0.3$ ,  $P = 0.002$ ) (Figure 8).

To understand the regulatory mechanism of miR-126 on VEGF pathway, the expression of PIK3R2 and SPRED1 (miR-126 targets in VEGF pathway) in virus and PBS groups were measured. The analysis of PIK3R2 expression indicated that in recombinant vector group expression of PIK3R2 was significantly reduced at days 14 and 21 compared with control group ( $0.06 \pm 0.04$ ,  $P = 0.05$ ,  $0.05 \pm 0.01$ ,  $P = 0.05$ , respectively) (Figure 9 A). Additionally expression of SPRED1 showed similar result to PIK3R2. In fact in virus group expression of SPRED1 was significantly reduced at days 14 and 21 compared with control group ( $0.06 \pm 0.02$ ,  $P = 0.02$ ,  $0.05 \pm 0.02$ ,  $P = 0.05$ , respectively) (Figure 9 B).

### **BM-MSCs<sup>miR-126</sup> transplantation improves angiogenesis in the ischemic hindlimb**

Gastrocnemius muscles were collected at days 7, 14, 21, and 28 after transplantation. In order to understand the angiogenic effect of recombinant vector, BM-MSCs and BM-MSCs<sup>miR-126</sup> in ischemic muscles at the cellular level, the gastrocnemius muscles were stained with H & E and the percentage of muscle regeneration was evaluated, in addition capillary density was assessed morphometrically by examining three fields per sections after immunofluorescence staining for endothelial cells with an anti-CD31 antibody. The analysis of muscle regeneration in gastrocnemius muscles indicated that muscles from BM-MSCs treated mice had a large increase in muscle regeneration compared with control group starting from day 14. BM-MSCs treated mice showed increased gastrocnemius muscle regeneration at days 14 and 21 ( $11.33 \pm 3.2$ ,  $P = 0.05$ ,  $18.66 \pm 7.09$ ,  $P = 0.08$ ). Results indicated that recombinant vector group compared to BM-MSCs group had similar effect on muscle regeneration and had great effect compared to control group. In fact gastrocnemius muscle regeneration was increased at days 14, 21 ( $12.6 \pm 2$ ,  $P = 0.04$ ,  $22 \pm 6$ ,  $P = 0.04$ ). BM-MSCs<sup>miR-126</sup> group showed significant gastrocnemius muscle regeneration compared to other groups, starting at day 7 from 11 % to 50 % at day 28 ( $10 \pm 1$ ,  $p < 0.0001$ ,  $19 \pm 4.1$ ,  $P = 0.001$ ,  $26.3 \pm 8.1$ ,  $P = 0.01$ ,  $45 \pm 15.6$ ,  $P = 0.02$ ) (Figure 10).

Results from IHC showed increased vasculature in BM-MSCs treated mice at days 14, 21, and 28 compared with control group ( $37.3 \pm 4.6$ ,  $P = 0.009$ ,  $45.6 \pm 4$ ,  $P = 0.008$ ,  $45 \pm 4.3$ ,  $P = 0.01$ , respectively). For recombinant vector group neoangiogenesis was increased at days 14, 21, and 28 compared with control group ( $40 \pm 4.5$ ,  $P = 0.002$ ,  $45.3 \pm 5.6$ ,  $P = 0.006$ ,  $46.3 \pm 4$ ,  $P = 0.002$ , respectively). BM-MSCs<sup>miR-126</sup> group showed significant vasculature compared to other groups, starting at day 7 and showed increased rate during 28 days ( $38.3 \pm 2.5$ ,  $45 \pm 2.6$ ,  $49.3 \pm 2.5$ ,  $51.6 \pm 3.5$ , respectively,  $P < 0.0001$  for all

time points). In fact CD31-MVD in BM-MSCs<sup>miR-126</sup> treated mice was significantly higher than the other groups (Figure 11).

## Discussion

Critical limb ischemia (CLI) considered as the most severe form of peripheral artery disease (PAD), being associated with a high risk of major amputation, cardiovascular events and death. CLI is considered the “end stage” of peripheral arterial disease (PAD). It is associated with considerable mortality, morbidity, and increased use of health care resources (33).

In this study we focused on the therapeutic neovascularization effect of BM-MSCs and microRNA-126 and combination use of them to provide insights into their potential for clinical use as a stem cell gene therapy for CLI.

At first step, BM-MSCs were isolated from Male C57BL/6 mice bone marrow. Then cells were assessed for MSCs CD markers and differentiation capacity. There are three criteria to define MSCs, in fact MSCs should exhibit some of these properties. 1) MSC must show fibroblast-like shape. 2) Expression of CD44, CD73, and CD90 and negative for CD14, CD34, and CD45. 3) The cells must be able to differentiate to adipocytes, osteocytes, and chondrocytes (34-36). The cells expressed MSC phenotypic markers. These typical MSC markers included CD34, CD45, CD44 and CD105. BM-MSCs were strongly positive for MSC marker CD44 and negative for cell markers CD105, CD34 and CD45. The results indicated that BM-MSCs successfully differentiated into osteocytes and adipocytes. After 2 weeks the cells showed calcium depositions and oil droplets in the cytoplasm and stained positive with alizarin red and oil red dye, respectively. These data demonstrated that BM-MSCs exhibited the characteristic MSC phenotypes.

In order to investigate the ability of BM-MSCs and BM-MSCs<sup>miR-126</sup> on endothelial cell migration, scratch assay was performed on the HUVEC cells. The results showed that 24 h after scratch initiation both BM-MSCs and BM-MSCs<sup>miR-126</sup> supernatant resulted in a significant percentage decrease in the scratch area remaining compared to the control group. Although BM-MSCs<sup>miR-126</sup> compared to BM-MSCs resulted in a faster closure of the wound. In fact both cells possess powerful paracrine effect on endothelial cell proliferation and migration. It is well known that MSCs perform their paracrine effects via secrete soluble factors which are angiogenic, anti-apoptotic, anti-inflammatory, and immunomodulatory. MSCs can secrete significant amounts of growth factors and cytokines that can promote new vessel formation and remodeling of injured tissues such as proangiogenic factors VEGF, bFGF, MMPs, IL-8 and HGF (37, 38). On the other hand one of the most important property of MSCs is their capacity for promoting angiogenesis, and proangiogenic factor VEGF is the main growth factor for this process that secret by MSCs during pathophysiological conditions (37, 39).

MiR-126 plays a critical role in regulating stem cell functions. MiR-126 can regulate the BM-MSCs proliferation, apoptosis, survival, migration, invasion, para-secretion and differentiation to endothelial cells via regulating the PI3K/AKT and MAPK/ERK1 signaling pathways. These pathways are an

intracellular signal transduction pathways that promote gene transcription, apoptosis, metabolism, proliferation, differentiation, cell survival, growth and angiogenesis in response to extracellular signals. Two important targets of miR-126 including PIK3R2 (P85 $\beta$ ) and SPRED1 play an important role as an inhibitor of PI3K (in PI3K/AKT signaling pathway) and RAF1 (in MAPK/ERK1 signaling pathway) respectively (40, 41). In BM-MSCs<sup>miR-126</sup>, miR-126 targets these two negative regulators of pathways and leading to promote signaling pathways that results in MSCs proliferation and increase paracrine secretion (42, 43). As a result, the BM-MSCs<sup>miR-126</sup> conditioned medium contains more effective concentration of angiogenic growth factors compared to untransformed MSCs, leads to increase remarkable proliferation and migration in human umbilical vein endothelial cells (HUVECs).

The BM-MSCs, recombinant vector and BM-MSCs<sup>miR-126</sup> were then assessed for their ability to treat critical limb ischemia. We used a model of limb ischemia that was induced by the complete removal of the femoral artery and the closing of its branches. At the first step, CLI induced mice were evaluated for functional recovery and ischemia using the Tarlov, ischemia, modified ischemia, function and the grade of limb necrosis scoring system at days 3, 7, 14, 21 and 28 after transplantation (33, 44). The results showed that BM-MSCs transplantation improved the treatment efficacy of hindlimb ischemia compared to control group. Remarkable improvements were observed in function and foot mobility with BM-MSCs treatment according to Tarlov and Function scores. In fact muscle function and muscle strength, which are a very important parameter to evaluate the angiogenic effects of MSCs therapy, improved during 28 days after BM-MSCs treatment. Additionally the mice showed restructuring of skeletal muscles at the injured sites and functional improvements. Mice in BM-MSCs group improved necrosis of the hindlimb and also showed reduced swelling and edema. In fact according to observational tests results, BM-MSCs compared to control group resulted in a faster and more effective recovery from limb ischemia because of its therapeutic properties. Recombinant vector treated mice showed similar effect to BM-MSCs group. But in BM-MSCs<sup>miR-126</sup> group functional improvements including muscle function and muscle strength and also restructuring of skeletal muscles were much better than the other groups.

In the next step, to evaluate angiogenesis at the cellular level, H&E and immunohistochemical staining was done for the evaluation of muscle regeneration and detection of CD31 endothelial cells marker. Assessment of neovascularization and capillary density was done by MVD score (45, 46). Results from H&E and IHC confirmed the results obtained from the behavioral tests. Muscle regeneration in BM-MSCs group had a significant increase compared to control group during 28 days, starting from day 14. On the other hand it confirmed that neovascularization and blood supply were increased at GC muscle. In recombinant vector group, similar effects to BM-MSCs group obtained. But BM-MSCs<sup>miR-126</sup> group showed significant increase in muscle regeneration compared to other groups. Furthermore IHC results indicated that formation of new blood vessels at day 7 was not significantly differ in BM-MSCs and recombinant vector groups, but at days 14, 21, and 28 neovascularization in 2 groups was greater than control groups. In BM-MSCs<sup>miR-126</sup> group according to MVD score neovascularization was increased after day 7 and significantly increased during 28 days compared to the other groups. According to results, MVD in BM-MSCs group was increased after day 14 compared with control group. This property of BM-

MSCs in promoting angiogenesis is related to the vascular differentiation capacity of these cells as well as secretion of angiogenic growth factors and cytokines (47, 48). In fact these results showed that histologic findings were associated with vascular and functional outcomes. On the other hand according to obtained results from behavioral, H&E, and IHC tests improvements were observed in muscle function and muscle strength with BM-MSCs treatment as well as formation of new blood vessels and muscle regeneration. BM-MSCs can contribute to angiogenesis via secretion of VEGF, angiogenin, IL-8, HGF, TNF-alpha, PD-ECGF, FGF-2, and MMP-9. VEGF plays a critical role in angiogenesis through stimulating endothelial cell proliferation, migration, and organization into tubules. Furthermore, VEGF can increase the number of circulating endothelial progenitor cells (49-52).

In BM-MSCs <sup>miR-126</sup> group these results (improvements in muscle function, muscle strength and formation of new blood vessels and muscle regeneration) was much better than in BM-MSCs group. As mentioned earlier, miR-126 can regulate PI3K/AKT and MAPK/ERK1 signaling pathways through targeting PIK3R2 and SPRED1. By inhibition of these two negative regulators, activation of pathways leads to MSCs proliferation, differentiation to ECs, increase paracrine secretion of angiogenic factors including VEGF, bFGF, and angiogenesis. In fact because of the angiogenic potential of miR-126, VEGF expression increases and consequently VEGF pathway and angiogenesis promotes (53, 54). In recombinant vector group, defined number of virus particles were injected intramuscularly (IM) at GC muscle. Consequently at skeletal muscle, miR-126 leads to increase VEGF expression and induces angiogenesis, muscle regeneration and functional improvements. In BM-MSCs <sup>miR-126</sup> group, the combination of angiogenic potential of BM-MSCs and miR-126 resulted in significant neovascularization, muscle regeneration and functional improvements compared to the other groups.

At day 28 after the treatment, the presence of donor cells were assessed by PCR for SRY gene. The results showed that both BM-MSCs and BM-MSCs <sup>miR-126</sup> were survived during 21 days at GC muscle and also BM-MSCs <sup>miR-126</sup> were detected at day 28. These results indicated important information concerning immunologic response after allogeneic MSC transplantation to the GC muscle. One of the most important limitations of MSCs transplantation to treat limb ischemia is poor survival of the transplanted cells because of adverse microenvironment in injured site such as hypoxia, ischemia and also excessive inflammation (55, 56). Previous studies demonstrated that BM-MSCs secrete various cytokines that have immunomodulatory, anti-inflammatory and anti-apoptotic functions in the target position of the transplantation such as IL-10, IL-6, PGE2 and TGF-  $\beta$  (57, 58). Some strategies are to reinforce the longevity of transplanted cells such as ways of delivery, number of injected cells, preconditioning of cells, genetic modification and combined cell therapy (59). In this study we used IM injection as delivery way and defined number of cells and also used miR-126 to increase the survival of BM-MSCs. According to the results these methods were effective in cell survival. MiR-126 can increase the resistance of the BM-MSCs to apoptosis via regulating the PI3K/AKT and MAPK/ERK1 signaling pathways. By inhibiting the negative regulators (PIK3R2 and SPRED1) of pathways, miR-126 increases the survival of the cells (31, 60).

Finally, the evaluation of VEGF expression in 4 groups showed that in BM-MSCs and virus groups VEGF over expression was similar but in miR-126-BM-MSCs group over expression of VEGF was remarkable. In BM-MSCs group over expression of VEGF is due to the paracrine effect of MSCs. MSCs have been extensively investigated as a source for promising proangiogenic cell therapy in angiogenesis dependent diseases such as CLI (61). BM-MSCs can secrete growth factors and cytokines related to angiogenesis such as VEGF. In virus group over expression of VEGF is due to the angiogenic potential of miR-126. As mentioned earlier, miR-126 targets two regulatory molecules (PIK3R2 and SPRED1) in PI3K/AKT and MAPK/ERK1 signaling pathways, leading to promote VEGF pathway and increasing secretion of VEGF (53, 62). On the other hand, miR-126 exerts angiogenic potential through regulating of stimulatory signaling pathways and inhibits the negative regulators.

It was demonstrated that both BM-MSCs and miR-126 have angiogenic potential. Therefore, to increase the angiogenic effect of MSCs, miR-126 was transferred to the cells and obtained results indicated that over expression of VEGF was higher than MSCs and virus groups separately. In other words, the angiogenic potential of BM-MSCs and miR-126 were combined together in order to achieve more effective therapy to treat CLI.

It was mentioned that miR-126 exerts angiogenic potential through inhibiting of PIK3R2 and SPRED1. In order to verify this regulatory mechanism, the expression of PIK3R2 and SPRED1 were evaluated in virus and control groups. Regulatory mechanism of miR-126 leads to decrease the expression of PIK3R2 and SPRED1 (31, 63). As expected, the expression of PIK3R2 and SPRED1 were decreased at days 14 and 21 in virus group compared to control group. Although the expression of PIK3R2 and SPRED1 on 28 day did not decrease as much as on 14 and 21 days. Additionally, the expression of VEGF in virus and MSCs groups on 28 day did not increase as much as on 14 and 21 days. It seems that after day 21, because of the progress in curing the disease (improvements in angiogenesis, muscle regeneration, muscle function, muscle strength and edema) and also decreased expression of miR-126, VEGF expression begins to decline and on the other hand the expression of PIK3R2 and SPRED1 begins to increase.

The purpose of this study was to investigate the potential of miR-126 on increasing angiogenic capacity as well as increasing BM-MSCs viability. According to the results, miR-126 has significant effect on mesenchymal stem cells functions to increase paracrine secretion, proliferation, differentiation, survival, migration and angiogenic potential.

## Conclusions

According to the obtained results, it can be concluded that combination use of BM-MSCs and miR-126 leads to more effective recovery from critical limb ischemia compared to using them alone. In fact, miR-126 due to its ability to regulate gene expression, especially genes involve in angiogenesis pathway, it can be used as a strong modifier to reinforce the angiogenic potential and survival of BM-MSCs, leading to more effective treatment for CLI.

## Abbreviations

CLI: Critical limb ischemia; PAD: Peripheral arterial disease; SCT: Stem cell therapy; BMMSCs: Bone marrow mesenchymal stem cells; MSCs: Mesenchymal stem cells; MiRNA: MicroRNA; VEGF: Vascular endothelial growth factor; SPRED1: Sprout-related EVH1 domain-containing protein 1; PIK3R2: Phosphoinositol-3 kinase regulatory subunit 2; LVs: Lentiviral vectors; GT: gene therapy; HIF-1: hypoxia inducible factor; SDF-1: Stromal Derived Factor-1; MMPs: matrix metalloproteinase; HUVECs: human umbilical vein endothelial cells.

## Declarations

### Acknowledgements

Not applicable.

### Authors' contributions

All authors contributed to the study conception and design. PN and LA performed all the experiments, collected, and analyzed the data. SD performed the animal surgery. JF designed the primers for real time PCR. PN wrote the manuscript. VR, and MT supervised the study. All authors read and approved the article.

### Funding

Not applicable.

### Availability of data and materials

All data generated or analyzed during this study are included in this published article.

### Ethics approval and consent to participate

All experimental procedures and use of research animals in this study were approved by the the Shiraz University of Medical Sciences ethics committee (1397.430).

### Consent for publication

Not applicable.

### Competing interests

The authors declare that they have no competing interests.

## References

1. Gerhard-Herman MD, Gornik HL, Barrett C, Barshes NR, Corriere MA, Drachman DE, et al. 2016 AHA/ACC guideline on the management of patients with lower extremity peripheral artery disease: executive summary: a report of the American College of Cardiology/American Heart Association Task Force on Clinical Practice Guidelines. *Journal of the American College of Cardiology*. 2017;69(11):1465-508.
2. Steffen MW, Undavalli C, Asi N, Wang Z, Elamin MB, Conte MS, et al. The natural history of untreated severe or critical limb ischemia. *Journal of vascular surgery*. 2015;62(6):1642-51. e3.
3. Steunenberg SL, Raats JW, Te Slaa A, de Vries J, van der Laan L. Quality of life in patients suffering from critical limb ischemia. *Annals of vascular surgery*. 2016;36:310-9.
4. Reinecke H, Unrath M, Freisinger E, Bunzemeier H, Meyborg M, Lüders F, et al. Peripheral arterial disease and critical limb ischaemia: still poor outcomes and lack of guideline adherence. *European heart journal*. 2015;36(15):932-8.
5. Hioki H, Miyashita Y, Miura T, Ebisawa S, Motoki H, Izawa A, et al. Prognostic improvement by multidisciplinary therapy in patients with critical limb ischemia. *Angiology*. 2015;66(2):187-94.
6. Pignon B, Sevestre M-A, Kanagaratnam L, Pernod G, Stephan D, Emmerich J, et al. Autologous Bone Marrow Mononuclear Cell Implantation and Its Impact on the Outcome of Patients With Critical Limb Ischemia—Results of a Randomized, Double-Blind, Placebo-Controlled Trial—. *Circulation Journal*. 2017;81(11):1713-20.
7. Poole J, Mavromatis K, Binongo JN, Khan A, Li Q, Khayata M, et al. Effect of progenitor cell mobilization with granulocyte-macrophage colony-stimulating factor in patients with peripheral artery disease: a randomized clinical trial. *Jama*. 2013;310(24):2631-9.
8. Fowkes FGR, Price JF. Gene therapy for critical limb ischaemia: the TAMARIS trial. *The Lancet*. 2011;377(9781):1894-6.
9. Han SW, Vergani Junior CA, Reis PEO. Is gene therapy for limb ischemia a reality? *Jornal Vascular Brasileiro*. 2020;19.
10. Han SW, Vergani Junior CA, Ocke Reis PE. Is gene therapy for limb ischemia a reality? *Jornal Vascular Brasileiro*. 2020;19.
11. Da Cunha FF, Martins L, Martin PKM, Stilhano RS, Gamero EJP, Han SW. Comparison of treatments of peripheral arterial disease with mesenchymal stromal cells and mesenchymal stromal cells modified with granulocyte and macrophage colony-stimulating factor. *Cytherapy*. 2013;15(7):820-9.
12. Khajeh S, Razban V, Talaei-Khozani T, Soleimani M, Asadi-Golshan R, Dehghani F, et al. Enhanced chondrogenic differentiation of dental pulp-derived mesenchymal stem cells in 3D pellet culture system: effect of mimicking hypoxia. *Biologia*. 2018;73(7):715-26.

13. Razban V, Khajeh S, Alaei S, Mostafavi-Pour Z, Soleimani M. Tube formation potential of BMSCs and USSCs in response to HIF-1 $\alpha$  overexpression under hypoxia. *Cytology and Genetics*. 2018;52(3):236-44.
14. Cortez-Toledo E, Rose M, Agu E, Dahlenburg H, Yao W, Nolte JA, et al. Enhancing retention of human bone marrow mesenchymal stem cells with pro-survival factors promotes angiogenesis in a mouse model of limb ischemia. *Stem cells and development*. 2019;28(2):114-9.
15. Petrenko Y, Vackova I, Kekulova K, Chudickova M, Koci Z, Turnovcova K, et al. A comparative analysis of multipotent mesenchymal stromal cells derived from different sources, with a focus on neuroregenerative potential. *Scientific reports*. 2020;10(1):1-15.
16. Razban V, Khajeh S, Lotfi AS, Mohsenifar A, Soleimani M, Khoshdel A, et al. Engineered heparan sulfate-collagen IV surfaces improve human mesenchymal stem cells differentiation to functional hepatocyte-like cells. *Journal of Biomaterials and Tissue Engineering*. 2014;4(10):811-22.
17. Fierro FA, Kalomoiris S, Sondergaard CS, Nolte JA. Effects on proliferation and differentiation of multipotent bone marrow stromal cells engineered to express growth factors for combined cell and gene therapy. *Stem Cells*. 2011;29(11):1727-37.
18. Altaner C, Altanerova V, Cihova M, Hunakova L, Kaiserova K, Klepanec A, et al. Characterization of mesenchymal stem cells of “no-options” patients with critical limb ischemia treated by autologous bone marrow mononuclear cells. *PLoS One*. 2013;8(9).
19. Nammian P, Asadi-Yousefabad S-L, Daneshi S, Sheikhha MH, Tabei SMB, Razban V. Comparative analysis of mouse bone marrow and adipose tissue mesenchymal stem cells for critical limb ischemia cell therapy. *Stem Cell Research & Therapy*. 2021;12(1):1-15.
20. Yamout B, Hourani R, Salti H, Barada W, El-Hajj T, Al-Kutoubi A, et al. Bone marrow mesenchymal stem cell transplantation in patients with multiple sclerosis: a pilot study. *Journal of neuroimmunology*. 2010;227(1-2):185-9.
21. Mohamed SA, Howard L, McInerney V, Hayat A, Krawczyk J, Naughton S, et al. Autologous bone marrow mesenchymal stromal cell therapy for “no-option” critical limb ischemia is limited by karyotype abnormalities. *Cytotherapy*. 2020.
22. Ferreira JR, Teixeira GQ, Santos SG, Barbosa MA, Almeida-Porada G, Gonçalves RM. Mesenchymal stromal cell secretome: influencing therapeutic potential by cellular pre-conditioning. *Frontiers in immunology*. 2018;9:2837.
23. Mao AS, Özkale B, Shah NJ, Vining KH, Descombes T, Zhang L, et al. Programmable microencapsulation for enhanced mesenchymal stem cell persistence and immunomodulation. *Proceedings of the National Academy of Sciences*. 2019;116(31):15392-7.

24. Zhang J, Sun X-J, Chen Ja, Hu ZW, Wang L, Gu DM, et al. Increasing the miR-126 expression in the peripheral blood of patients with diabetic foot ulcers treated with maggot debridement therapy. *Journal of Diabetes and its Complications*. 2017;31(1):241-4.
25. Kulshreshtha R, Ferracin M, Wojcik SE, Garzon R, Alder H, Agosto-Perez FJ, et al. A microRNA signature of hypoxia. *Molecular and cellular biology*. 2007;27(5):1859-67.
26. Dang LT, Lawson ND, Fish JE. MicroRNA control of vascular endothelial growth factor signaling output during vascular development. *Arteriosclerosis, thrombosis, and vascular biology*. 2013;33(2):193-200.
27. Caporali A, Emanuelli C. MicroRNA regulation in angiogenesis. *Vascular pharmacology*. 2011;55(4):79-86.
28. Nammian P, Razban V, Tabei SMB, Asadi-Yousefabad S-L. MicroRNA-126: Dual Role in Angiogenesis Dependent Diseases. *Current pharmaceutical design*. 2020.
29. Zhou J, Li Y-S, Nguyen P, Wang K-C, Weiss A, Kuo Y-C, et al. Regulation of vascular smooth muscle cell turnover by endothelial cell–secreted microRNA-126: role of shear stress. *Circulation research*. 2013;113(1):40-51.
30. Li Y, Tian L, Sun D, Yin D. Curcumin ameliorates atherosclerosis through upregulation of miR-126. *Journal of cellular physiology*. 2019.
31. Fish JE, Santoro MM, Morton SU, Yu S, Yeh R-F, Wythe JD, et al. miR-126 regulates angiogenic signaling and vascular integrity. *Developmental cell*. 2008;15(2):272-84.
32. van Solingen C, Seghers L, Bijkerk R, Duijs JM, Roeten MK, van Oeveren-Rietdijk AM, et al. Antagomir-mediated silencing of endothelial cell specific microRNA-126 impairs ischemia-induced angiogenesis. *Journal of cellular and molecular medicine*. 2009;13(8a):1577-85.
33. Krishna SM, Omer SM, Li J, Morton SK, Jose RJ, Golledge J. Development of a two-stage limb ischemia model to better simulate human peripheral artery disease. *Scientific reports*. 2020;10(1):1-16.
34. Dominici M, Le Blanc K, Mueller I, Slaper-Cortenbach I, Marini F, Krause D, et al. Minimal criteria for defining multipotent mesenchymal stromal cells. The International Society for Cellular Therapy position statement. *Cytotherapy*. 2006;8(4):315-7.
35. Pham LH, Vu NB, Van Pham P. The subpopulation of CD105 negative mesenchymal stem cells show strong immunomodulation capacity compared to CD105 positive mesenchymal stem cells. *Biomedical Research and Therapy*. 2019;6(4):3131-40.
36. Lv F-J, Tuan RS, Cheung KM, Leung VY. Concise review: the surface markers and identity of human mesenchymal stem cells. *Stem cells*. 2014;32(6):1408-19.

37. Maacha S, Sidahmed H, Jacob S, Gentilcore G, Calzone R, Grivel J-C, et al. Paracrine mechanisms of mesenchymal stromal cells in angiogenesis. *Stem cells international*. 2020;2020.
38. Watt SM, Gullo F, van der Garde M, Markeson D, Camicia R, Khoo CP, et al. The angiogenic properties of mesenchymal stem/stromal cells and their therapeutic potential. *British medical bulletin*. 2013;108(1):25-53.
39. Tao H, Han Z, Han ZC, Li Z. Proangiogenic features of mesenchymal stem cells and their therapeutic applications. *Stem cells international*. 2016;2016.
40. Chen J-J, Zhou S-H. Mesenchymal stem cells overexpressing MiR-126 enhance ischemic angiogenesis via the AKT/ERK-related pathway. *Cardiology journal*. 2011;18(6):675-81.
41. Kong R, Gao J, Ji L, Zhao D. MicroRNA-126 promotes proliferation, migration, invasion and endothelial differentiation while inhibits apoptosis and osteogenic differentiation of bone marrow-derived mesenchymal stem cells. *Cell Cycle*. 2020;19(17):2119-38.
42. Chang L, Liang J, Xia X, Chen X. miRNA-126 enhances viability, colony formation, and migration of keratinocytes HaCaT cells by regulating PI3 K/AKT signaling pathway. *Cell biology international*. 2019;43(2):182-91.
43. Sheng L, Mao X, Yu Q, Yu D. Effect of the PI3K/AKT signaling pathway on hypoxia-induced proliferation and differentiation of bone marrow-derived mesenchymal stem cells. *Experimental and therapeutic medicine*. 2017;13(1):55-62.
44. Kang I, Lee B-C, Choi SW, Lee JY, Kim J-J, Kim B-E, et al. Donor-dependent variation of human umbilical cord blood mesenchymal stem cells in response to hypoxic preconditioning and amelioration of limb ischemia. *Experimental & molecular medicine*. 2018;50(4):1-15.
45. Hu W, Jiang J, Yang F, Liu J. The impact of bone marrow-derived mesenchymal stem cells on neovascularisation in rats with brain injury. *Folia Neuropathol*. 2018;56:112-23.
46. Li GC, Zhang HW, Zhao QC, Sun L, Yang JJ, Hong L, et al. Mesenchymal stem cells promote tumor angiogenesis via the action of transforming growth factor  $\beta$ 1. *Oncology letters*. 2016;11(2):1089-94.
47. Wu Y, Chen L, Scott PG, Tredget EE. Mesenchymal stem cells enhance wound healing through differentiation and angiogenesis. *Stem cells*. 2007;25(10):2648-59.
48. Trivanović D, Jauković A, Popović B, Krstić J, Mojsilović S, Okić-Djordjević I, et al. Mesenchymal stem cells of different origin: comparative evaluation of proliferative capacity, telomere length and pluripotency marker expression. *Life Sciences*. 2015;141:61-73.

49. Shen C-C, Chen B, Gu J-T, Ning J-L, Chen L, Zeng J, et al. The angiogenic related functions of bone marrow mesenchymal stem cells are promoted by CBDL rat serum via the Akt/Nrf2 pathway. *Experimental cell research*. 2016;344(1):86-94.
50. Wang J, Wang Y, Wang S, Cai J, Shi J, Sui X, et al. Bone marrow-derived mesenchymal stem cell-secreted IL-8 promotes the angiogenesis and growth of colorectal cancer. *Oncotarget*. 2015;6(40):42825.
51. Fam NP, Verma S, Kutryk M, Stewart DJ. Clinician guide to angiogenesis. *Circulation*. 2003;108(21):2613-8.
52. Ullah M, Liu DD, Thakor AS. Mesenchymal stromal cell homing: mechanisms and strategies for improvement. *Iscience*. 2019;15:421-38.
53. Ye L, Peng Y, Mo J, Yao Y. MiR-126 enhances VEGF expression in induced pluripotent stem cell-derived retinal neural stem cells by targeting spred-1. *International Journal of Clinical and Experimental Pathology*. 2018;11(2):1023.
54. Qu Q, Bing W, Meng X, Xi J, Bai X, Liu Q, et al. Upregulation of miR-126-3p promotes human saphenous vein endothelial cell proliferation in vitro and prevents vein graft neointimal formation ex vivo and in vivo. *Oncotarget*. 2017;8(63):106790.
55. Li X, Zhou J, Liu Z, Chen J, Lü S, Sun H, et al. A PNIPAAm-based thermosensitive hydrogel containing SWCNTs for stem cell transplantation in myocardial repair. *Biomaterials*. 2014;35(22):5679-88.
56. Tano N, Kaneko M, Ichihara Y, Ikebe C, Coppens SR, Shiraishi M, et al. Allogeneic mesenchymal stromal cells transplanted onto the heart surface achieve therapeutic myocardial repair despite immunologic responses in rats. *Journal of the American Heart Association*. 2016;5(2):e002815.
57. Saldaña L, Bensiamar F, Vallés G, Mancebo FJ, García-Rey E, Vilaboa N. Immunoregulatory potential of mesenchymal stem cells following activation by macrophage-derived soluble factors. *Stem cell research & therapy*. 2019;10(1):1-15.
58. Weiss ARR, Dahlke MH. Immunomodulation by mesenchymal stem cells (MSCs): mechanisms of action of living, apoptotic, and dead MSCs. *Frontiers in Immunology*. 2019;10:1191.
59. Araña M, Gavira JJ, Peña E, González A, Abizanda G, Cilla M, et al. Epicardial delivery of collagen patches with adipose-derived stem cells in rat and minipig models of chronic myocardial infarction. *Biomaterials*. 2014;35(1):143-51.
60. Chen L, Wang J, Wang B, Yang J, Gong Z, Zhao X, et al. MiR-126 inhibits vascular endothelial cell apoptosis through targeting PI3K/Akt signaling. *Annals of hematology*. 2016;95(3):365-74.

61. Bronckaers A, Hilkens P, Martens W, Gervois P, Ratajczak J, Struys T, et al. Mesenchymal stem/stromal cells as a pharmacological and therapeutic approach to accelerate angiogenesis. *Pharmacology & therapeutics*. 2014;143(2):181-96.
62. Qu M-J, Pan J-J, Shi X-J, Zhang Z-J, Tang Y-H, Yang G-Y. MicroRNA-126 is a prospective target for vascular disease. *Neuroimmunology and Neuroinflammation*. 2018;5.
63. Ji J-S, Xu M, Song J-J, Zhao Z-W, Chen M-J, Chen W-Q, et al. Inhibition of microRNA-126 promotes the expression of Spred1 to inhibit angiogenesis in hepatocellular carcinoma after transcatheter arterial chemoembolization: in vivo study. *OncoTargets and therapy*. 2016;9:4357.

## Tables

Table 1: Functional scales

Tarlov score	Description
0	No movement
1	Barely perceptible movement, non-weight bearing
2	Frequent movement, non-weight bearing
3	Supports weight, partial weight bearing
4	Walks with mild deficit
5	Normal but slow walking
6	Full and fast walking
Ischemia score	Description
0	Autoamputation > half lower limb
1	Gangrenous tissue > half foot
2	Gangrenous tissue < half foot, with lower limb muscle necrosis
3	Gangrenous tissue < half foot, without lower limb muscle necrosis
4	Pale foot or gait abnormalities
5	Normal
Modified ischemia score	Description
0	Autoamputation of leg
1	Leg necrosis
2	Foot necrosis
3	Discoloration of 2 toes
4	Discoloration of 1 toe
5	Discoloration of > 2 nails
6	Discoloration of 1 nail
7	No necrosis
The grade of limb necrosis	Description
0	Normal limb without swelling, necrosis or atrophy of muscle

1	Necrosis limiting to toes (toes loss)
2	Necrosis extending to a dorsum pedis (foot loss)
3	Necrosis extending to a crus (knee loss)
4	Necrosis extending to a thigh (total hind-limb loss)
Function score	Description
0	Dragging
1	No plantar flexion
2	No toe flexion
3	No grabbing force
4	Some grabbing force
5	Normal

Table 2: Primers used for quantitative real-time PCR

GAPDH forward	5'-CTGTGGGCAAGGTCATCCCAGAG-3'
GAPDH reverse	5'-CTTCTTGATGTCATCATACTTGGCAGGTT-3'
VEGF forward	5'-TACCTCCACCATGCCAAGTG-3'
VEGF reverse	5'-AAGATGTCCACCAGGGTCTC-3'
PIK3R2 forward	5'-GCTTCTCAGAGCCCCTTACCTTCTG-3'
PIK3R2 reverse	5'-GTCCTCCTTCACCACCTGGTCTTGT-3'
SPRED1 forward	5'-ACTTCCCGTTCCTAGTGAAAGATCAC-3'
SPRED1 reverse	5'-AGCCTTGCTGACTGAATGGTATCTGG-3'

## Figures

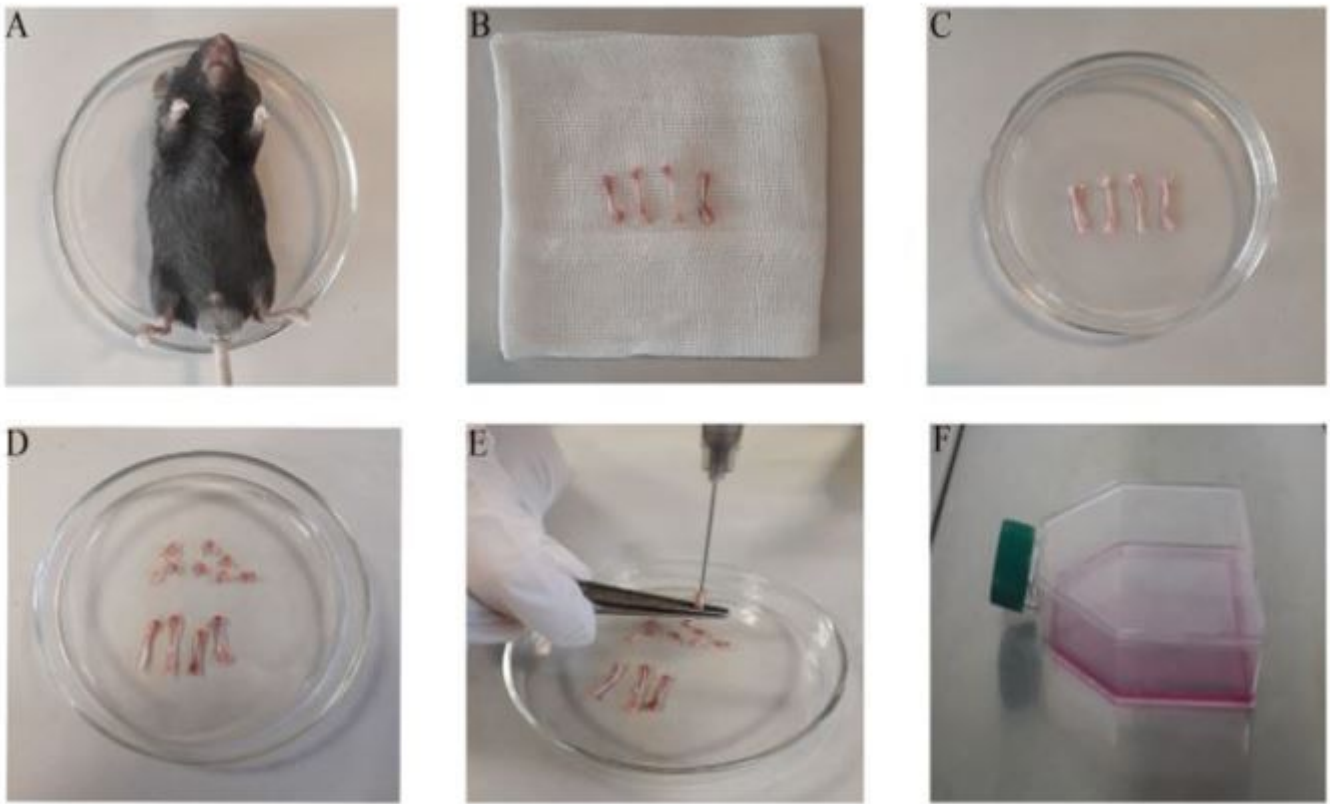


**Figure 1**

Images of bone marrow derived mesenchymal stem cell collection procedures (A) First the mouse was sacrificed by cervical dislocation (B) Tibia and femur bones were dissected and then muscles, ligaments, and tendons were removed (C) Bones were transferred to a 100-mm sterile culture dish with 5 mL phosphate-buffered saline containing penicillin–streptomycin (D) The dish was transferred into the biosafety cabinet and the two ends of bones below the end of the marrow cavity were cut with scalpel (E) A 5-ml syringe was inserted into the bone cavity and used to slowly flush the marrow out. The bone cavities were washed until the bones became pale. (F) Finally all the bone pieces were removed and the media transferred to a new flask that incubated at 37C in a 5% CO<sub>2</sub> incubator (G).

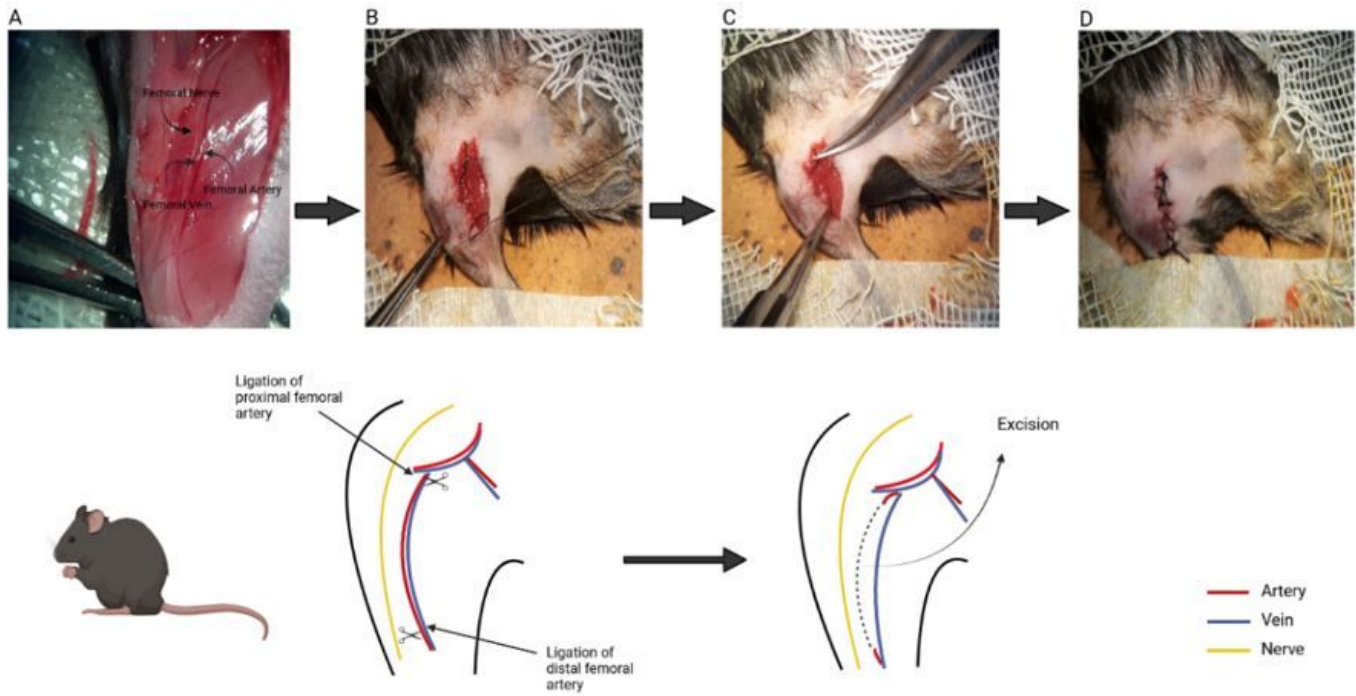


**Figure 2**

Procedure for creating the critical limb ischemia mouse model. Total excision of femoral artery was performed. Determination of femoral artery, vein and nerve (A) Ligation of proximal and distal femoral artery (B) Total excision of femoral artery (C) and suturing the surgical site (D).

A

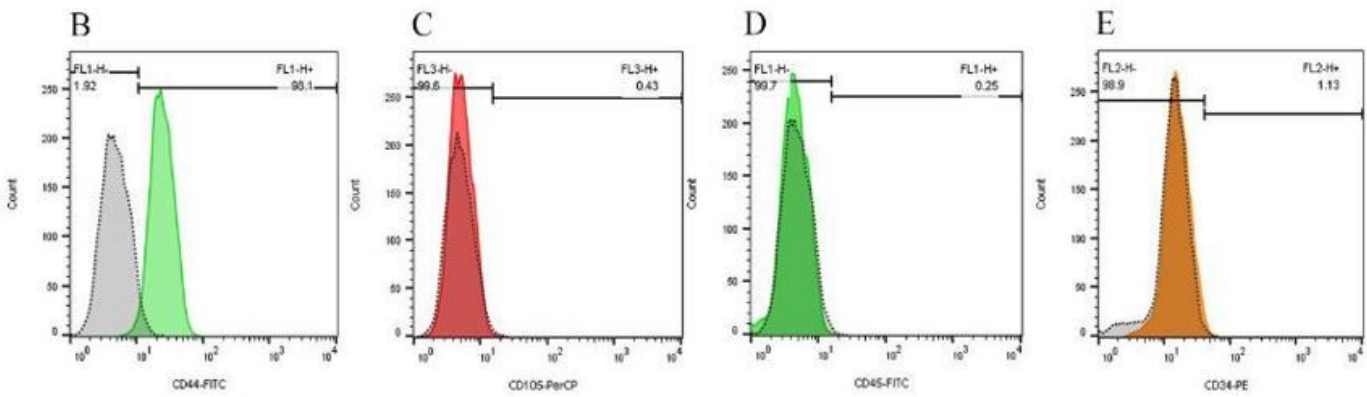
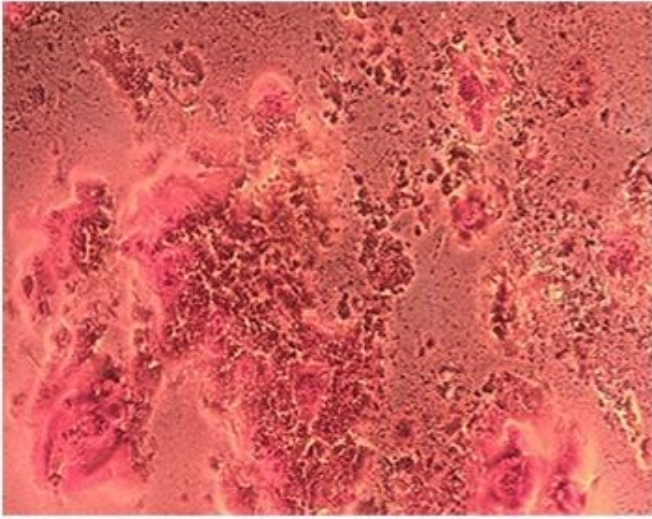


**Figure 3**

Morphology of bone marrow mesenchymal stem cells (A) under inverted microscope (10 $\times$ ) and Cell surface markers expression of C57BL/6 mice bone marrow mesenchymal stem cells. Flow cytometry analysis results showed that BM-MSCs were positive for MSC marker CD44 (B) and negative for CD105 (C). Cells were negative for haematopoietic cell marker CD45 (D) and CD34 (E).

Osteogenesis (A)



Adipogenesis (B)

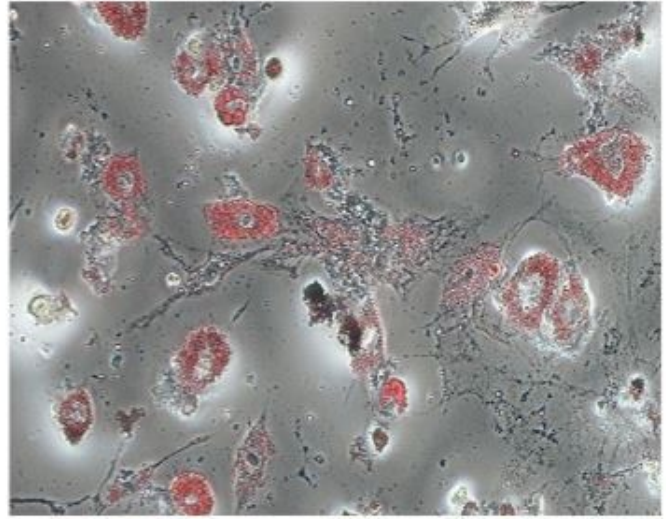


**Figure 4**

Differentiation capacity of mouse bone marrow mesenchymal stem cells (BM-MSCs). BM-MSCs with the ability to differentiate into osteoblasts (A) and adipocytes (B).

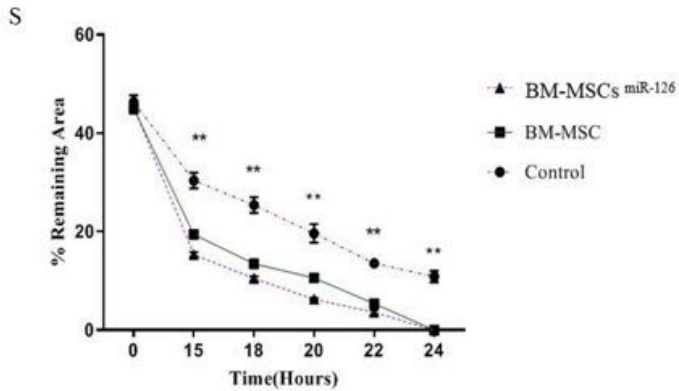
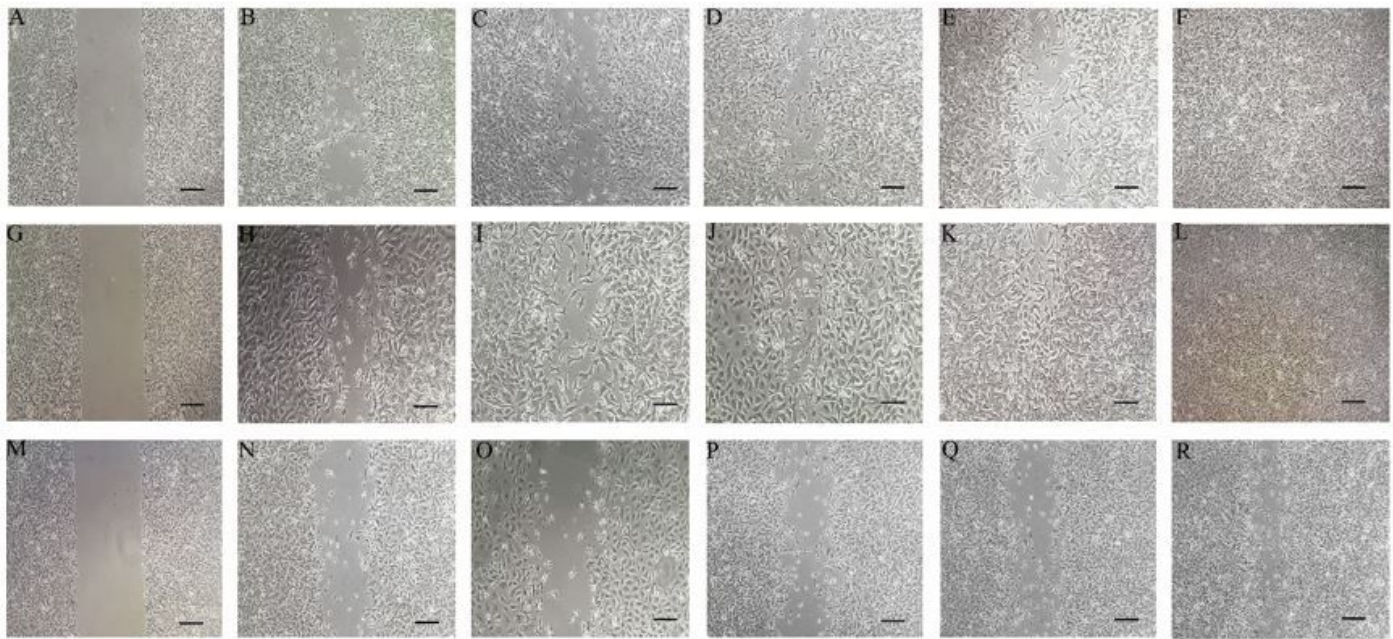


**Figure 5**

For BM-MSCs conditioned medium, the images in a time series (T0, T15, T18, T20, T22, T24) were analyzed for gap area over time (A-F). For BM-MSCs miR-126 conditioned medium, the images in the same time series were analyzed (G-L). Photomicrographs from the control group in a defined time series (M-R). Graphical comparison of the mean ingrowth and standard deviation (SD) of control, BM-MSCs and BM-MSCs miR-126 groups. P values  $\leq 0.05$  were considered statistically significant (\* $p < 0.05$ , \*\* $p < 0.01$ , \*\*\* $p < 0.001$ , \*\*\*\* $p < .0001$ ). (s). Magnification 10 $\times$ , Scale bar, 200  $\mu\text{m}$ .

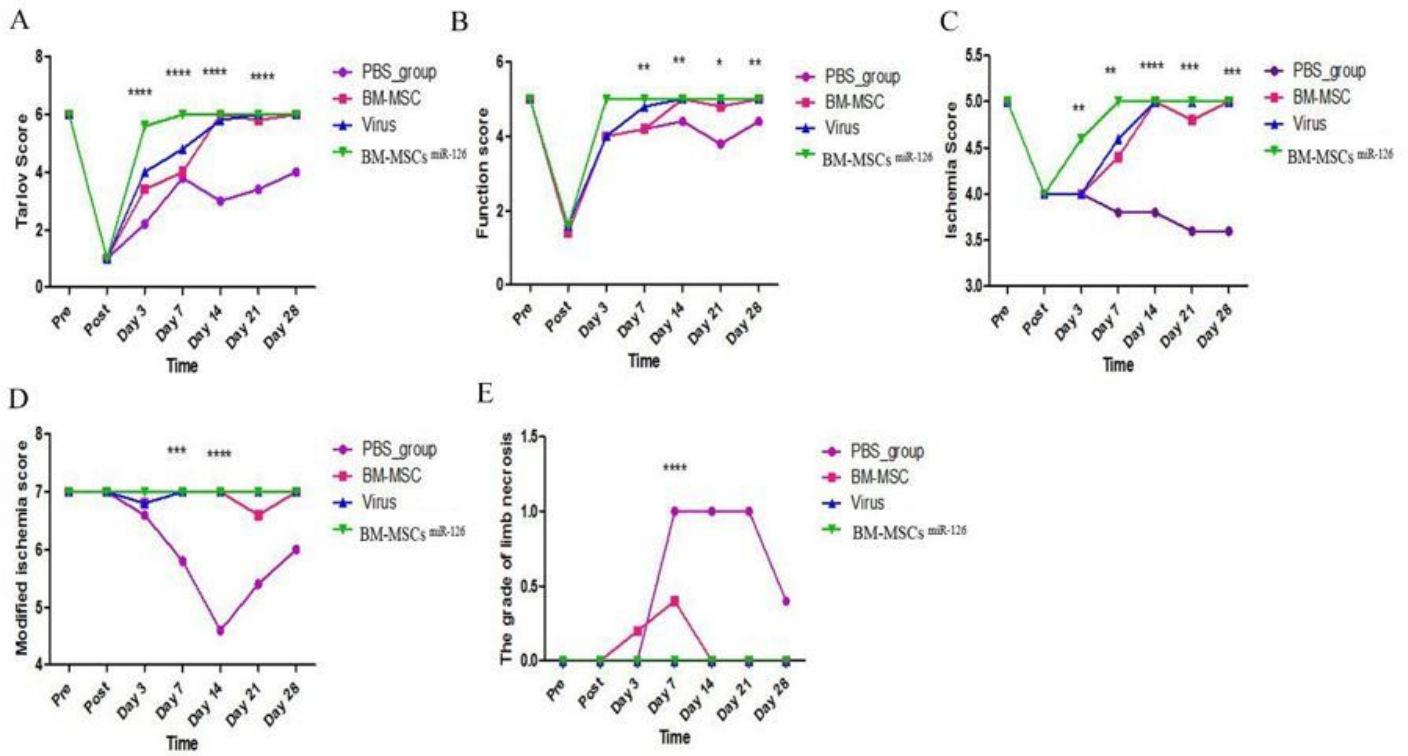


**Figure 6**

Functional scoring. All transplanted mice groups were evaluated for functional recovery according to Tarlov score and Function score (A-B). Evaluation of ischemia was performed by ischemia score and modified ischemia score (C-D). And improvements of necrotic changes was determined according to the grade of limb necrosis score (E). Data presented as (mean  $\pm$  SD) ( $P \leq 0.05$ ) (\* $p < 0.05$ , \*\* $p < 0.01$ , \*\*\* $p < 0.001$ , \*\*\*\* $p < .0001$ ).

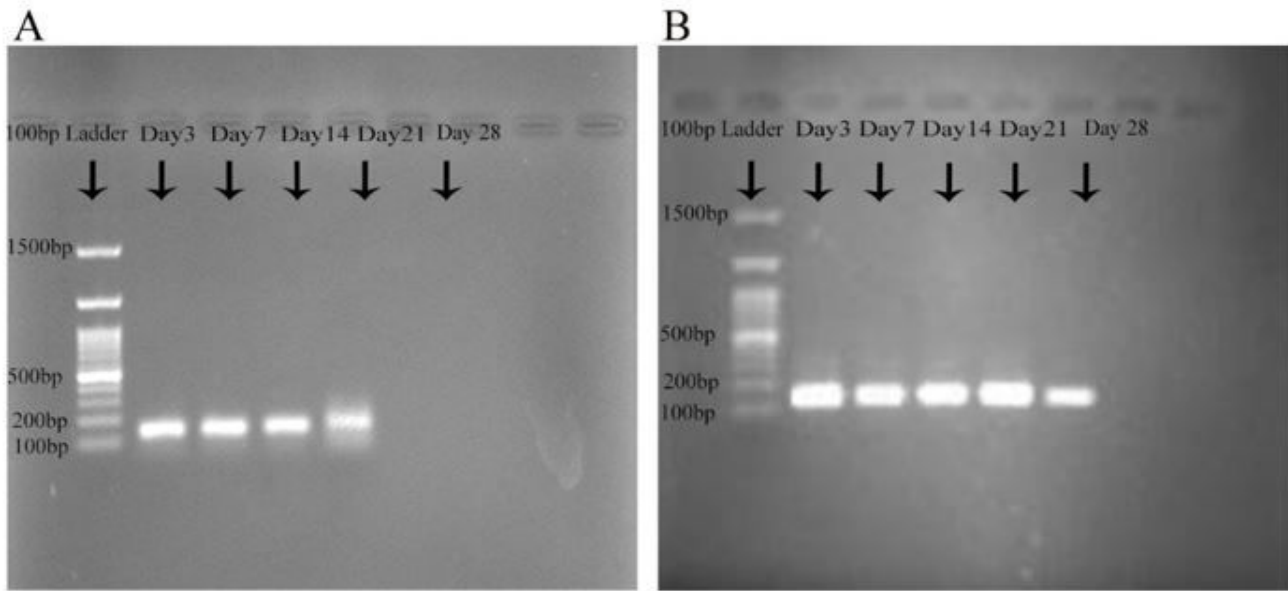


**Figure 7**

PCR for SRY gene. BM-MSCs (A) and BM-MSCs miR-126 cells (B).

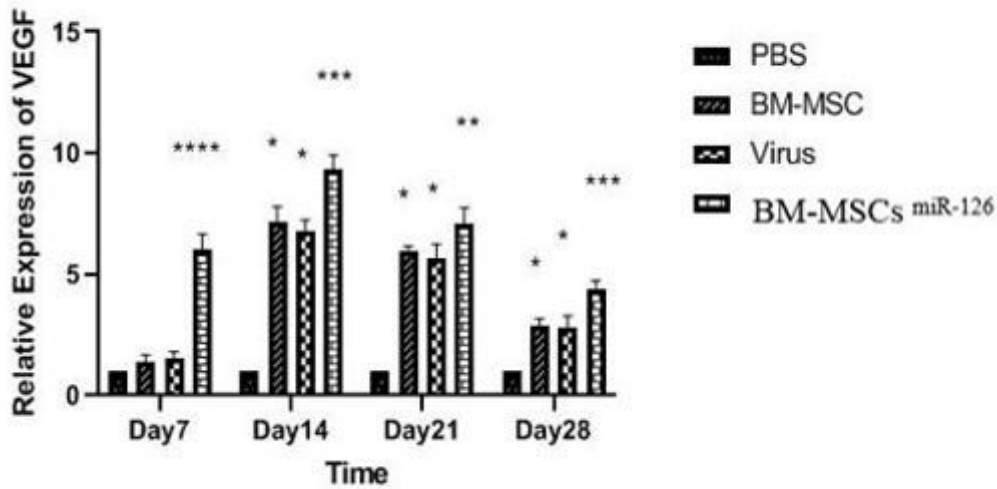


**Figure 8**

Relative gene expression of VEGF. mRNA levels of VEGF was determined in PBS, BM-MSCs, Virus, and BM-MSCs miR-126 groups. The expression of VEGF was significantly higher in the BM-MSCs miR-126 group compared with other groups. Results are expressed as (mean  $\pm$  SD) ( $P \leq 0.05$ ).

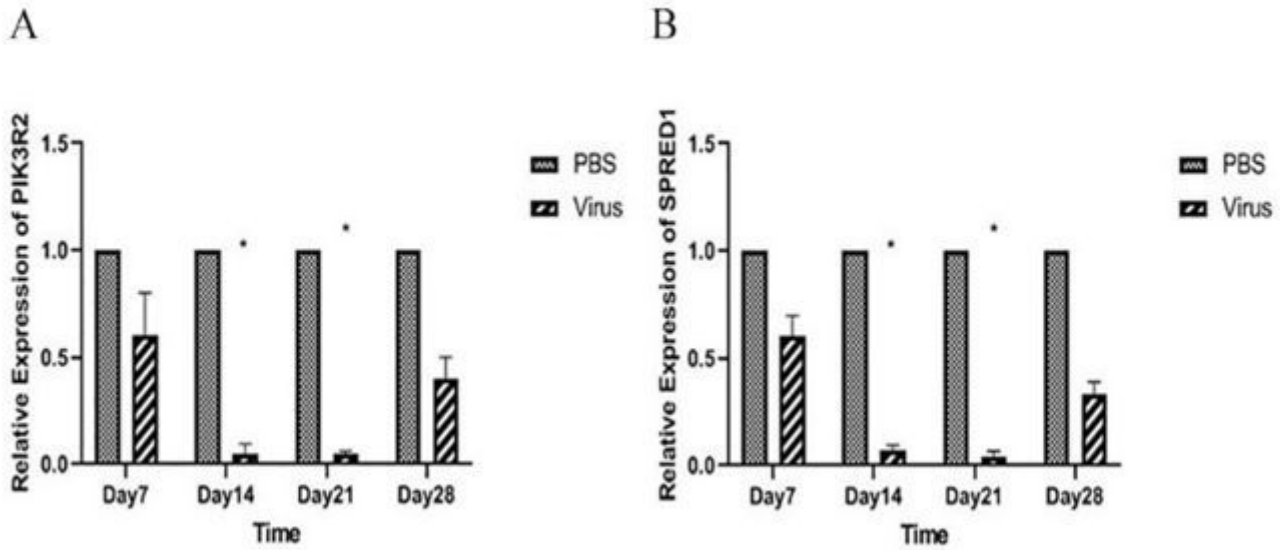


**Figure 9**

Relative gene expression of PIK3R2 and SPRED1. The expression of PIK3R2 (A) and SPRED1 (B) were determined in PBS and Virus groups. The expression of PIK3R2 and SPRED1 were significantly decreased in Virus groups. Data are presented as (mean  $\pm$  SD) ( $P \leq 0.05$ ) (\* $p < 0.05$ , \*\* $p < 0.01$ , \*\*\* $p < 0.001$ , \*\*\*\* $p < .0001$ ).

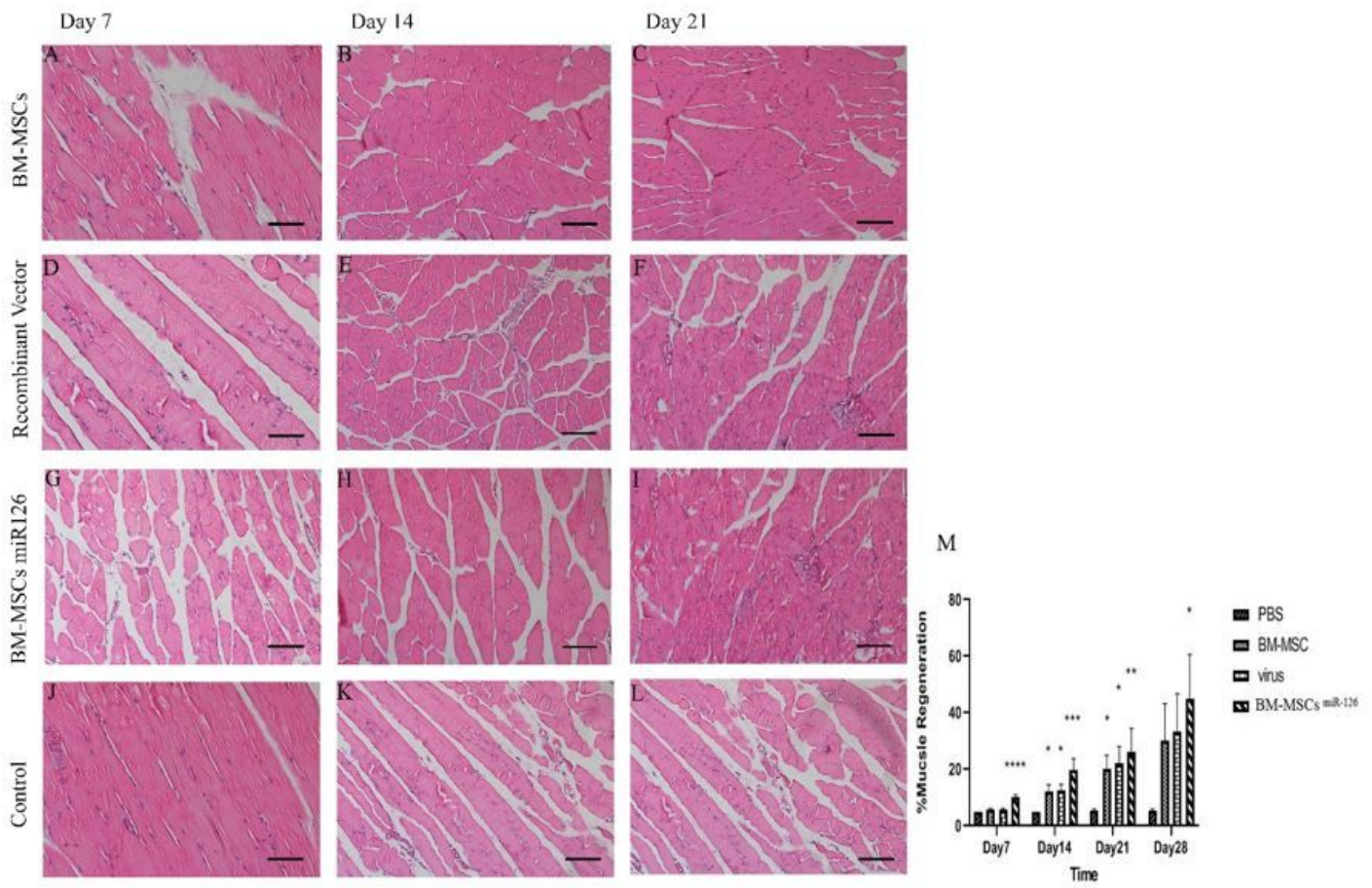


**Figure 10**

Histological analysis after H&E staining. Gastrocnemius muscle regeneration characterized by the presence of centrally located nucleus in mice treated with BM-MSCs (A-C), recombinant vector (D-F) BM-MSCs miR-126 (G-I) and control group (J-L) at days 7, 14 and 21. Quantification of the percentage (mean  $\pm$  SD) of muscle regeneration ( $P \leq 0.05$ ) (\* $p < 0.05$ , \*\* $p < 0.01$ , \*\*\* $p < 0.001$ , \*\*\*\* $p < .0001$ ). (M). Magnification 100 $\times$ , Scale bar, 50  $\mu\text{m}$ .

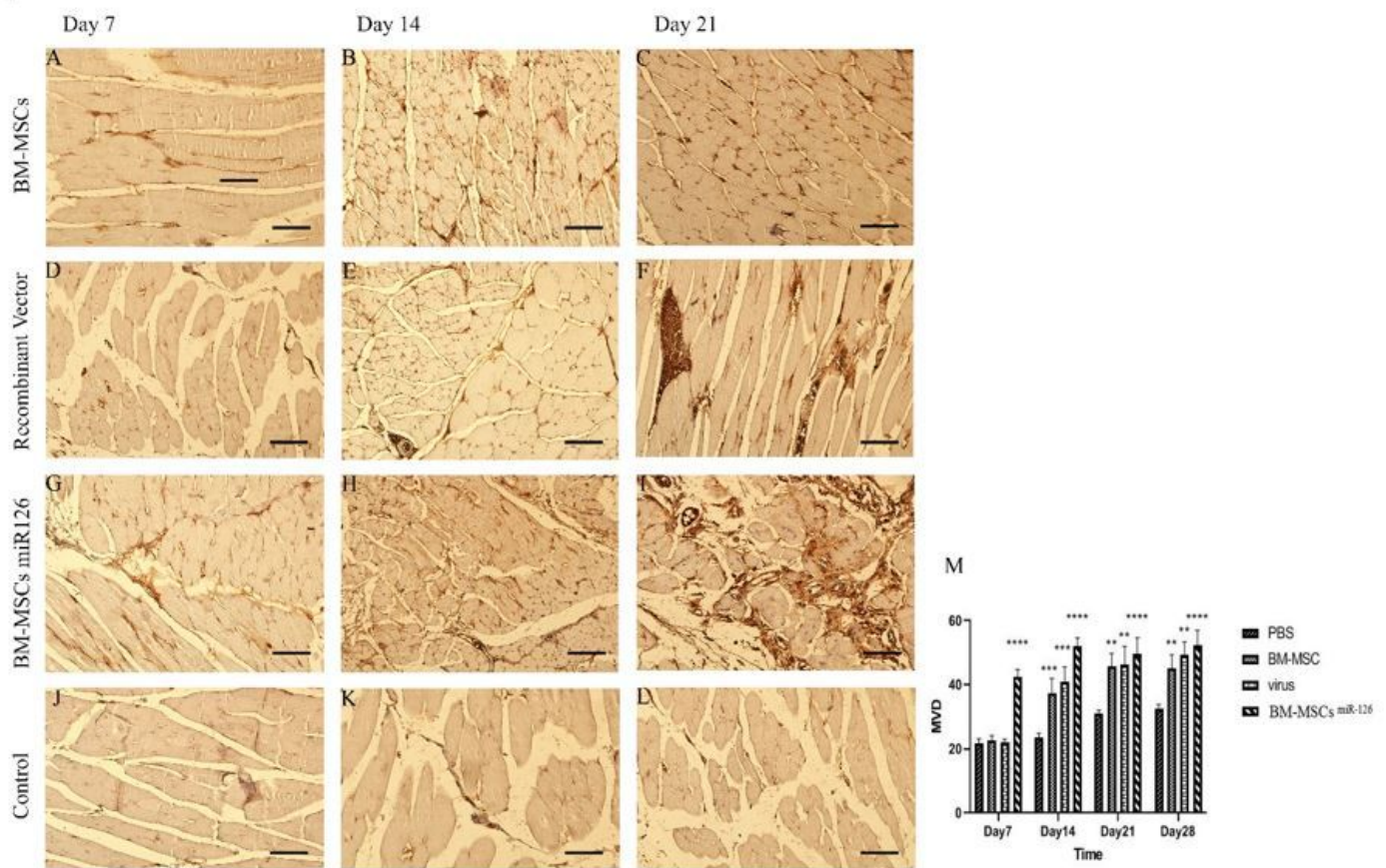


**Figure 11**

Histological analysis of limb muscles. Immunohistochemical staining of BM-MSCs (A-C) recombinant vector (D-F) BM-MSCs miR-126 (G-I) and control groups (J-L) with anti-CD31 antibody at days 7, 14 and 21. Quantification of capillary density. Capillary density was counted after CD31 staining. Data presented as (mean  $\pm$  SD) ( $P \leq 0.05$ ) (\* $p < 0.05$ , \*\* $p < 0.01$ , \*\*\* $p < 0.001$ , \*\*\*\* $p < .0001$ ). (M). Magnification 100 $\times$ , Scale bar, 50  $\mu\text{m}$ .